Selective transport of Cu(II), Co(II), Cd(II) and Ni(II) ions through polymer inclusion membranes (PIMs) based on some amide derivatives of 4-amino-1,5-dimethyl-2-phenylpyrazolidin-3-one

A.F. Shaaban*, M.M. Azab, A.A. Mahmoud, A.A. Khalil, A.M. Metwally

Chemistry Department, Faculty of Science, Benha University, Benha, Egypt, Tel. +20 1091174238; email: afshaaban@hotmail.com (A.F. Shaaban), Tel. +20 1009437694; email: drmorsy2000@yahoo.com (M.M. Azab), Tel. +20 1221792651; email: amal.mahmoud90@yahoo.com (A.A. Mahmoud), Tel. +20 1063029888; email: aamkhalil55@yahoo.com (A.A. Khalil), Tel. +20 1094636335; email: amal.chemistry@yahyoo.com (A.M. Metwally)

a b s t r a c t

A new polymer inclusion membranes (PIMs) doped with amide derivatives of 4-amino-1,5-dimethyl-2-phenylpyrazolidin-3-one [*N*-(1,5-dimethyl-3-oxo-2-phenylpyrazolidin-4-yl)dodecanamide (*N*-PYDA), *N*-(1,5-dimethyl-3-oxo-2-phenylpyrazolidin-4-yl)tetradecanamide (*N*-PYTA), *N*-(1,5-dimethyl-3-oxo-2-phenylpyrazolidin-4-yl)palmitamide (*N*-PYPA) and *N*-(1,5-dimethyl-3-oxo-2-phenylpyrazolidin-4-yl)stearamide (*N*-PYSA)] as fixed carriers, cellulose triacetate (CTA) as base polymer and dioctyl phthalate as a plasticizer have been prepared. The studied carriers were prepared by the reaction of fatty acids (stearic, palmitic, myristic and lauric acid) with 4-amino-1,5-dimethyl-2-phenylpyrazolidin-3-one in the presence of *N,N′*-dicyclohexylcarbodiimide as dehydrating agent. The chemical structure of the prepared carriers was confirmed by Fourier transform infrared (FTIR) and nuclear magnetic resonance (^{1}H NMR), while the prepared membranes were characterized using different techniques such as FTIR, X-ray diffraction and scanning electron microscopy. The selective transport of Cu(II), Co(II), Cd(II) and Ni(II) ions through PIM was investigated and optimized as a function of transport time, pH, membrane composition, type of receiving phase and its concentration. Results showed that the alkyl chain length has an effect on the transport rate of Cu(II), Co(II), Cd(II) and Ni(II) ions through the CTA membranes. The obtained results show that around 90% of Cu(II) was transported from the source phase containing equimolar mixture of all metal ions at pH 5.2 through PIM after 7 h into 3.0 M HCl using carrier (*N*-PYSA). The best results of normalized initial flux and recovery are obtained for membranes containing 40% of all carriers.

Keywords: Polymer inclusion membrane; Dioctyl phthalate; Cellulose triacetate; *N,N′*-dicyclohexylcarbodiimide; Amide derivatives of pyrazolidin-3-one

1. Introduction

The separation and removal of toxic metal ions and neutral chemicals from water has frequently been discussed in membrane technology. Several kinds of liquid membranes have been used; among them polymer inclusion membrane (PIM) has been evolved which provides metal ion transport with high selectivity [1].

PIMs called plasticized polymer membranes [2] have attracted considerable interest during the last few years due to their advantages over the most commonly used liquid membranes, i.e., emulsion liquid membranes and supported liquid membranes in the metal ion transport, such as long-term stability, a high selectivity, low cost, low energy consumption and an easy setup. Also, PIMs have higher chemical stability and mechanical resistance [3,4].

Actually, PIMs mainly focused on their application on metal cations transport such as copper [5–7], zinc [8–10], lead [4,10,11], cadmium [4,10] and others [12–15]. Many papers have been shown that this type of membranes is able

* Corresponding author.

to transport different metal cations with high selectivity and characterizing by good process efficiency. A few publications also report the application of PIMs in the transport of organic compounds such as carbohydrates [16,17], amino acids [17–19], organic acids [17,20,21] and others [17,22]. In these papers, received results are comparable with results obtained for metal cations transport show that PIMs are able to transport both the inorganic and organic compounds on the same level.

The objective of the present work is to prepare a novel PIMs (based on cellulose triacetate [CTA] as base polymer, dioctyl phthalate [DOP] as plasticizer and some new amide derivatives of 4-amino-1,5-dimethyl-2-phenylpyrazolidin-3-one as a new fixed carriers) and use them for the selective extraction of copper, cobalt, cadmium and nickel cations. We compared the behavior of the prepared carriers toward competitive transport of Cu(II), Co(II), Cd(II) and Ni(II) ions through a prepared membrane at different operating conditions such as type of carrier and its wt%, contact time, pH of source and receiving phases.

2. Experimental and characterization techniques

PIMs are prepared by a solution containing an extractant (carrier), a plasticizer and a base polymer such as CTA or poly(vinyl chloride), which forms a thin, flexible and stable film. However, in the last years other polymers were reported for PIM's preparation, i.e., cellulose acetate propionate, cellulose acetate butyrate and cellulose tributyrate [23]. The polymer presents as an interconnected support network, while the carrier supports the species transportation.

2.1. Materials

Analytical grade inorganic chemical copper(II), cobalt(II), cadmium(II) and nickel(II) chlorides were obtained from Fluka. Organic reagents: CTA, DOP, fatty acids (stearic, palmitic, myristic and lauric acid), *N,N'*-dicyclohexylcarbodiimide (DCC) and 4-aminoantipyrine (4-amino-1,5-dimethyl-2-phenylpyrazolidin-3-one) were purchased from Fluka (USA) and used without further purification. Dichloromethane (CH_2Cl_2) was purchased from Sigma-Aldrich, Co. USA. Deionized water was used for preparing all aqueous solutions.

2.2. Synthesis

2.2.1. Synthesis of carriers

0.02 mol fatty acid (stearic, palmitic, myristic or lauric acid) was dissolved in 25 mL of dichloromethane. Solution of 0.01 mol DCC (2.06 g) in 25 mL of dichloromethane was added to above solution with stirring for 15 min. The mixture was filtered off to remove dicyclohexyl urea. 0.01 mol of 4-amino-antipyrine (2.03 g) dissolved in 50 mL dichloromethane was added to the filtrate and stirred for 2 h. The product [*N*-(1,5-dimethyl-3-oxo-2-phenylpyrazolidin-4-yl)dodecanamide (*N*-PYDA), *N*-(1,5-dimethyl-3-oxo-2-phenylpyrazolidin-4-yl)tetradecanamide (*N*-PYTA), *N*-(1,5-dimethyl-3-oxo-2-phenylpyrazolidin-4-yl)palmitamide (*N*-PYPA) and *N*-(1,5-dimethyl-3-oxo-2-phenylpyrazolidin-4-yl)stearamide (*N*-PYSA)] was obtained by evaporating dichloromethane and the solid product washed with petroleum ether to remove liberated acid. Crystallization with benzene, melting point 120°C and yield 83%.

2.2.2. Membrane preparation

The membranes were prepared according to the procedure reported in the previous paper [24]. A solution of CTA (0.1 g dissolved in 10 mL dichloromethane) as the base polymer, 0.1 mL of DOP as plasticizer and 0.3 g of carrier in 10 mL of dichloromethane was stirred to obtain a transparent solution. This solution was poured into a Petri dish of a 6.0 cm diameter. After slow solvent evaporation overnight, the resulting membrane was peeled off from the Petri dish by immersion in cold water. Then, the membrane was soaked for 12 h in distilled water to achieve their homogeneity.

2.3. Characterization techniques

2.3.1. Fourier transform infrared (FTIR) measurements

The IR spectra for prepared carriers and membranes were measured using FT/IR-BRUKER, Vector 22 (Germany) Spectrophotometer.

2.3.2. Nuclear magnetic resonance spectra (¹H NMR)

The proton magnetic resonance spectra (in $CDCl_3$ as a solvent) for prepared carriers were recorded on Bruker 400 MHz spectrophotometer. The chemical shift (δ) is given downfield relative to tetramethylsilane as internal standard.

2.3.3. Scanning electron microscopy (SEM)

Scanning electron microscopy was used to show the surface morphology of the prepared membranes. Micrographs were obtained using (QUANTA 250 SEG, HOLANDA) microanalyzer microscope.

2.3.4. X-ray diffraction (XRD)

The X-ray diffraction (XRD) of the prepared membranes were obtained from Diano X-ray diffractometer using Cu Kα radiation ($\lambda = 1.5418$ Å).

2.3.5. Determination of the metal ions concentration

Metal ions concentration was determined by using Hitachi atomic absorption Z-6100 polarized Zeeman spectrometer.

2.4. Transport studies

Transport studies were carried out in a permeation cell in which the membrane film (at the surface area of 7.06 cm²) was tightly clamped between two cells. Both the source and receiving aqueous phases (160 mL each) were stirred at 800 rpm. The source phase was solution containing chlorides of Cu(II), Co(II), Cd(II) and Ni(II) ions at the concentration of 0.01 M for each metal. The receiving phase was 1.0 M aqueous solution of hydrochloric acid. The PIM transport studies were carried out at room temperature. Small samples (1 mL each) of the source and receiving phase were taken periodically using a sampling port with a syringe and analyzed to determine metal ions

concentrations by atomic absorption spectroscopy method. The pH of source phase was controlled by pH meter and kept constant by adding few drops of NaOH aqueous solution.

The kinetics of the PIM transport were described by a first-order transport rate equation in metal ion concentration:

$$\ln\left[\frac{c}{c_i}\right] = -kt \tag{1}$$

where c is the concentration (M) of metal ion in the source phase at given time, c_i is initial metal ion concentration (M) in the source phase, k is rate constant (s⁻¹) and t is time of metal transport (s).

To calculate the k values, plots of $\ln(c/c_i)$ with time were drawn. The rate constant value for the duplicate transport experiment was averaged and standard deviation was calculated and edited in Table 3. The relationship of $\ln(c/c_i)$ vs. time was linear, which was confirmed by high values of correlation coefficient (R^2), i.e., which were mostly from 0.863 to 0.993.

Permeability coefficient P (m/s) can be determined:

$$P = \frac{V}{A} \cdot k \tag{2}$$

The initial flux (J_i) was determined as equal to:

$$J_i = \frac{V}{A} \cdot k \cdot c_i \tag{3}$$

where V is volume of the source phase (m³) and A is area of the effective membrane (m²).

The selectivity coefficient S was known as the ratio of the initial fluxes for M_1 and M_2 metal ions, respectively:

$$S = J_{iM1}/J_{iM2} \tag{4}$$

The removal % (R) of metal ions from the source phase into receiving phase was calculated as:

$$R = \frac{c_i - c}{c_i} \cdot 100\% \tag{5}$$

3. Results and discussion

Coupling of fatty acids (stearic, palmitic, myristic and lauric acid) with 4-aminoantipyrine in the presence of DCC to afford the corresponding amide was shown in Fig. 1.

3.1. Characterization of prepared carriers

3.1.1. FTIR spectra of prepared carriers

Figs. 2(a)–(d) show FTIR spectra of the prepared carriers, which shown absorption peaks for all carriers at 1,690 cm⁻¹ attributed to C=O of amide in five-membered rings and band at 1,650 cm⁻¹ for C=O of amide in fatty chain. The band at 3,241 cm⁻¹ assigned to NH group. The bands at 2,850 and 2,920 cm⁻¹ can be assigned to CH₂ group symmetry and asymmetry of fatty chain, respectively.

3.1.2. ¹H NMR spectra of prepared carriers

Table 1 represents the chemical shift (δ) of the prepared carriers in ¹H NMR spectra.

3.2. Membranes characteristic

3.2.1. FTIR spectra of prepared membranes

The membranes CTA + plasticizer + carriers were characterized using FTIR.

Fig. 3 showed the spectra of the different prepared membranes. Table 2 collected the peak values and the corresponding radical of the reference CTA, DOP and CTA + DOP + carriers membranes.

The obtained results showed that all the maximum values obtained from the spectrum of the CTA reference membrane, i.e., without plasticizer and carrier, are present in the prepared membranes spectra in addition to those of the carrier molecules. This result confirms the presence of plasticizer and carrier in the polymer matrix.
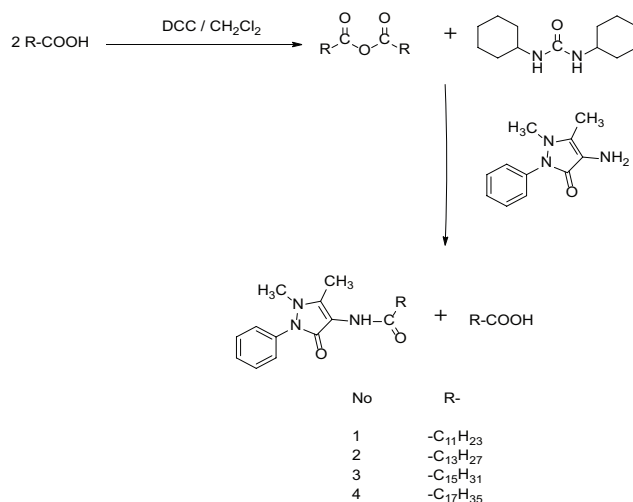

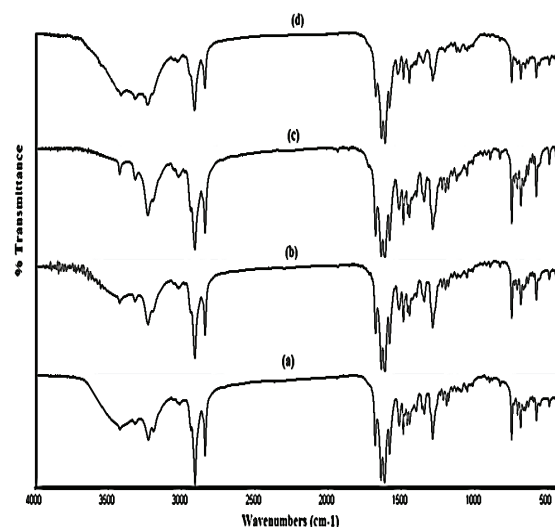Fig. 1. The reaction of 4-aminoantipyrine with fatty acids.

Fig. 2. FTIR spectra of the prepared carriers: (a) carrier *N*-PYDA, (b) carrier *N*-PYTA, (c) carrier *N*-PYPA and (d) carrier *N*-PYSA.

Table 1
The collected data of ^{1}H NMR of the prepared carriers

Carrier	δ (ppm)	Corresponding radical
N-PYDA	0.853	(3H, **CH**$_3$)
	1.435	(16H, **CH**$_2$ of fatty chain of lauric acid)
	1.75	(2H, CO − **C** − **CH**$_2$)
	2.3	(3H, **CH**$_3$–C=C–)
	2.4	(2H, CO**CH**$_2$)
	3.1	(3H, **CH**$_3$–N–)
	7.3–7.6	(5H, **CH** aromatic)
	8.6	(1H, N**H**), which D$_2$O exchangeable
N-PYTA	0.853	(3H, **CH**$_3$)
	1.435	(20H, **CH**$_2$ of fatty chain of myristic acid)
	1.75	(2H, CO − **C** − **CH**$_2$)
	2.3	(3H, **CH**$_3$–C=C–)
	2.4	(2H, CO**CH**$_2$)
	3.1	(3H, **CH**$_3$–N–)
	7.3–7.6	(5H, **CH** aromatic)
	8.3	(1H, N**H**), which D$_2$O exchangeable
N-PYPA	0.853	(3H, **CH**$_3$)
	1.435	(24H, **CH**$_2$ of fatty chain of palmitic acid)
	1.75	(2H, CO − **C** − **CH**$_2$)
	2.3	(3H, **CH**$_3$–C=C–)
	2.4	(2H, CO**CH**$_2$)
	3.1	(3H, **CH**$_3$–N–)
	7.3–7.6	(5H, **CH** aromatic)
	8.3	(1H, N**H**), which D$_2$O exchangeable
N-PYSA	0.853	(3H, **CH**$_3$)
	1.435	(28H, **CH**$_2$ of fatty chain of stearic acid)
	1.75	(2H, CO − **C** − **CH**$_2$)
	2.3	(3H, **CH**$_3$–C=C–)
	2.4	(2H, CO**CH**$_2$)
	3.1	(3H, **CH**$_3$–N–)
	7.3–7.6	(5H, **CH** aromatic)
	8.6	(1H, N**H**), which D$_2$O exchangeable

Fig. 3. FTIR spectra of the prepared membranes: (a) CTA + DOP + carrier (*N*-PYDA), (b) CTA + DOP + carrier (*N*-PYTA), (c) CTA + DOP + carrier (*N*-PYPA) and (d) CTA + DOP + carrier (*N*-PYSA).

Table 2
Peak values and the corresponding radicals in different membranes

Membrane	Peak value (cm^{-1})	Corresponding radical
CTA	3,450–5,550	O–H
	2,935	C–H
	1,739	C=O
	1,526	COO$^-$
DOP	1,726	C=O stretching of (COO)
	1,077	C–O stretching of O–CH$_2$
	1,285	C–O stretching of O=C–O
CTA + DOP + carriers	Same peaks of CTA and DOP	
(*N*-PYDA,	1,690 and 1,650	2 C=O (carrier)
N-PYTA,	2,850	C–H (carrier) symmetry
N-PYPA and	2,920	C–H (carrier) asymmetry
N-PYSA)	3,241	NH (carrier)

take place. As a result, the whole membrane is available for transport [27–29].

3.2.2. X-ray diffraction

Fig. 4 shows the X-ray curves for CTA + plasticizer + carriers membranes. Based on these figures, we can observe the following:

- The CTA membrane presents a single maximum at approximately 20° found in all polymers and corresponds to the van der Waals halo [25,26]. Thus, this material presents basically amorphous characteristics.
- The systems constituted by the mixture of CTA + DOP + carriers do not give any diffraction. It can be due to the absence of crystalline structure of the membrane which permits us to eliminate the mechanism of transfer of the ions by successive jumps between carrier complexing sites. PIMs can be viewed as non-porous and as discussed in the SEM section, there is no convincing evidence of a microchannel network in which metal ion transport can
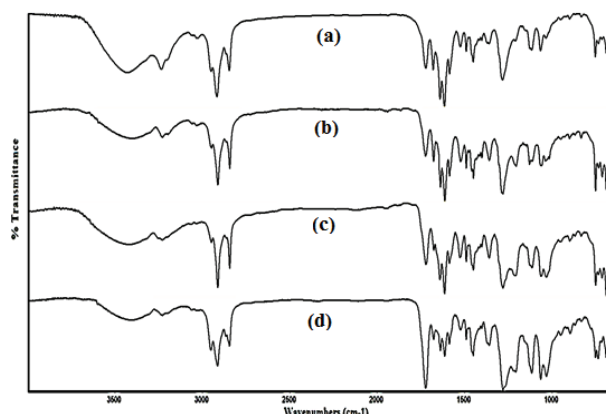
3.2.3. Characterization by scanning electron microscopy (SEM)

The morphologies of the CTA + plasticizer + carriers membranes (cross-section; Figs. 5(a)–(d)) show that the CTA–plasticizer (DOP) and carriers membranes present a dense structure where the pores of membrane have been filled by the DOP and carriers molecules yielding a thick and less porous membrane.

3.3. Transport factors

3.3.1. Effect of transport time

Transport time is important role for copper(II), cobalt(II) cadmium(II) and nickel(II) transport because various
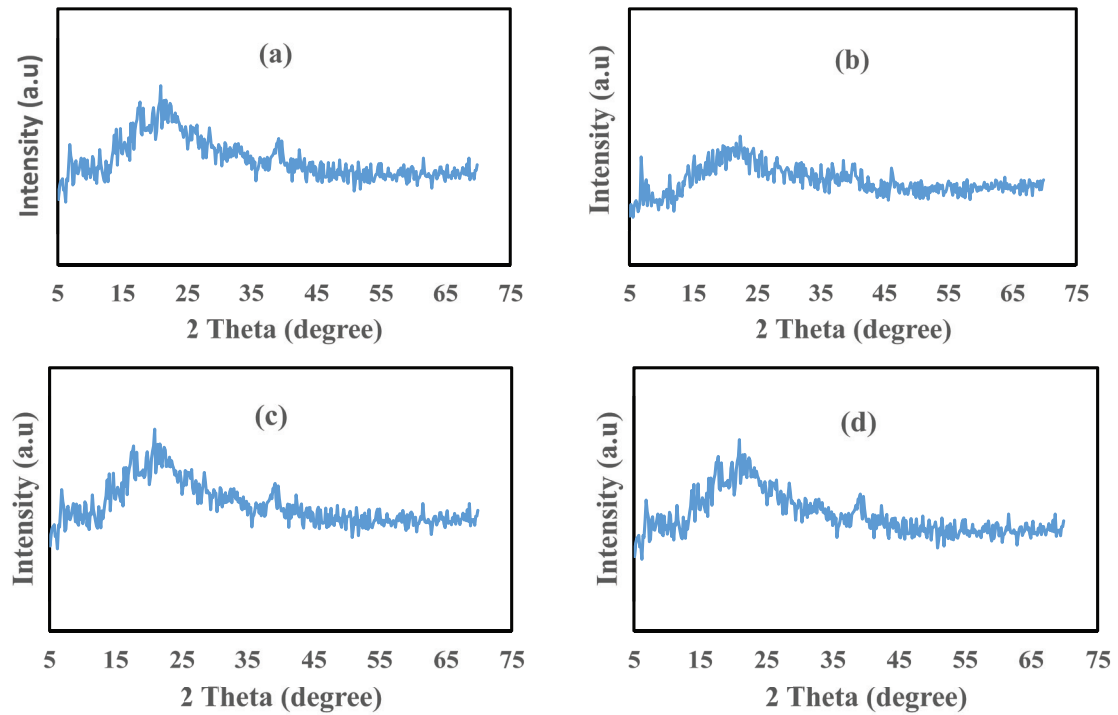
Fig. 4. X-ray diffraction of the prepared membranes: (a) CTA + DOP + carrier (*N*-PYDA), (b) CTA + DOP + carrier (*N*-PYTA), (c) CTA + DOP + carrier (*N*-PYPA) and (d) CTA + DOP + carrier (*N*-PYSA).
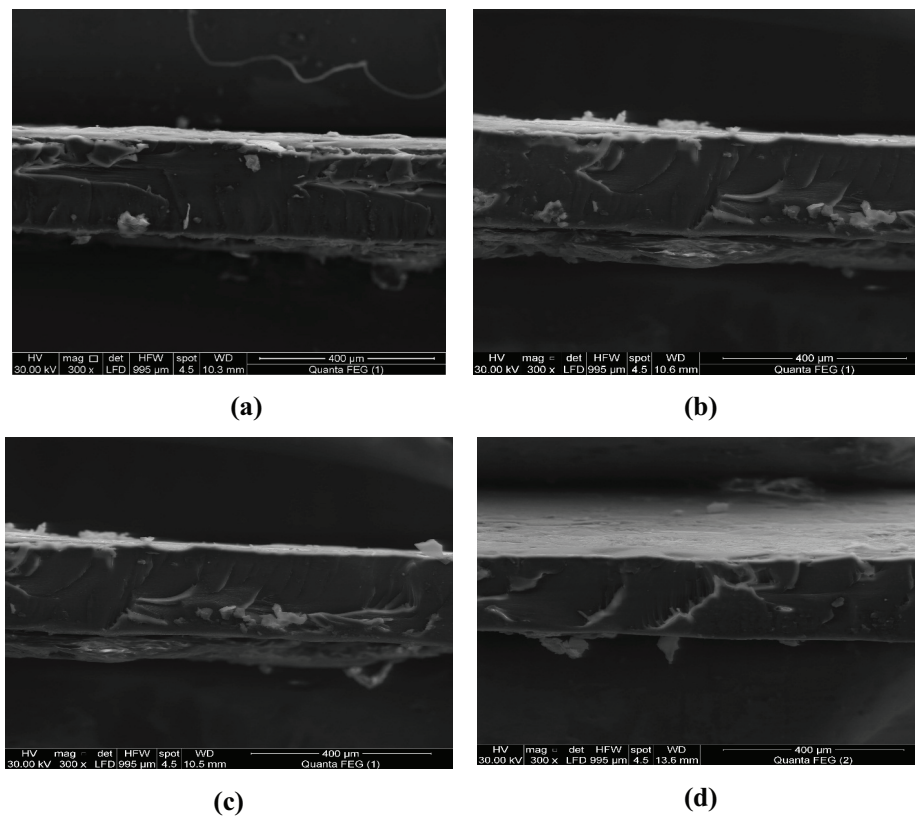

Fig. 5. Scanning electron microscopy of various membranes: (a) CTA + DOP + carrier (*N*-PYDA), (b) CTA + DOP + carrier (*N*-PYTA), (c) CTA + DOP + carrier (*N*-PYPA) and (d) CTA + DOP + carrier (*N*-PYSA).

transport time can give information about mass transfer, kinetic reaction, membrane permeability and flux. To investigate the effect of transport time on copper(II), cobalt(II) cadmium(II) and nickel(II) transport, the Cu(II), Co(II), Cd(II) and Ni(II) transport were investigated at various transport time. The carrier is a complexing agent, which chemically interacts with the species from the aqueous solution as shown in Fig. 6.

As it could be seen, transport rate depends on used carrier. The initial fluxes and selectivity coefficients of copper(II), cobalt(II), cadmium(II) and nickel(II) ions transport across PIMs using different carriers from aqueous source phase of equimolar mixture of all metals are shown in Table 3 and Fig. 7. The copper(II) ions were transported with a highest rate and the selectivity order was as follows: Cu(II) > Co(II) > Cd(II) > Ni(II). The initial flux of copper(II) transport increased with different carriers in the order: *N*-(1,5-dimethyl-3-oxo-2-phenylpyrazolidin-4-yl)dodecanamide (*N*-PYDA) < *N*-(1,5-dimethyl-3-oxo-2-phenylpyrazolidin-4-yl)tetradecanamide

(*N*-PYTA) < *N*-(1,5-dimethyl-3-oxo-2-phenylpyrazolidin-4-yl)palmitamide (*N*-PYPA) < *N*-(1,5-dimethyl-3-oxo-2-phenylpyrazolidin-4-yl)stearamide (*N*-PYSA). The observed trend is in accordance with increasing length of alkyl fatty chain in the corresponding carrier. On the basis of obtained results, it could be noticed that carriers with alkyl chain length from 12 to 18 carbon atoms are able to fast transport of examined copper(II), cobalt(II) cadmium(II) and nickel(II) ions through PIM. The maximum value of the initial flux for Cu(II) ions was equal to 6.8×10^{-5} mol/m^2 s (for carrier *N*-PYSA).

3.3.2. Effect of pH

Fig. 8 showed the effect of pH of source phase on copper, cobalt, cadmium and nickel ions transport through PIMs using different carriers. The concentration of copper, cobalt, cadmium and nickel ions remaining in the source phase was measured at different pH ranging from 1.2 to 5.2. The results
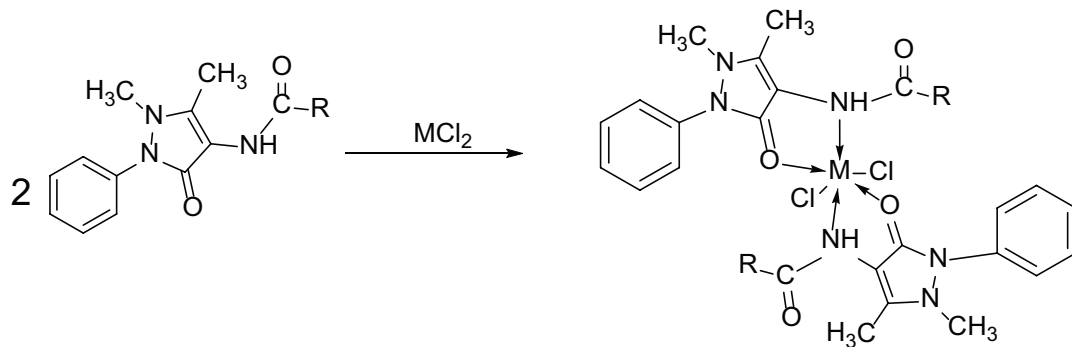

Fig. 6. Structure of metal complexes with carrier.

Table 3
Initial flux and selectivity coefficients for competitive transport of Cu(II), Co(II), Cd(II) and Ni(II) ions across PIMs

Carrier	Metal ions	$k \times 10^5$ (s^{-1})	$J_i \times 10^5$ (mol/m^2 s)	$S_{Cu(II)/Me(II)}$		
N-PYDA	Cu(II)	2.4 ± 0.214	5.4	Cu(II) > Co(II) > Cd(II) > Ni(II)		
	Co(II)	1.1 ± 0.079	2.5	2.2	3.4	6.0
	Cd(II)	0.7 ± 0.083	1.6			
	Ni(II)	0.4 ± 0.070	0.9			
N-PYTA	Cu(II)	2.5 ± 0.170	5.7	Cu(II) > Co(II) > Cd(II) > Ni(II)		
	Co(II)	1.2 ± 0.101	2.7	2.1	3.2	5.2
	Cd(II)	0.8 ± 0.079	1.8			
	Ni(II)	0.5 ± 0.086	1.1			
N-PYPA	Cu(II)	2.7 ± 0.178	6.1	Cu(II) > Co(II) > Cd(II) > Ni(II)		
	Co(II)	1.3 ± 0.088	3.0	2.0	2.7	4.4
	Cd(II)	1.0 ± 0.095	2.3			
	Ni(II)	0.6 ± 0.071	1.4			
N-PYSA	Cu(II)	3.0 ± 0.107	6.8	Cu(II) > Co(II) > Cd(II) > Ni(II)		
	Co(II)	1.6 ± 0.063	3.6	1.9	2.7	4.3
	Cd(II)	1.1 ± 0.105	2.5			
	Ni(II)	0.7 ± 0.066	1.6			

Conditions: Source phase: $c_{Me} = 0.01$ M, pH = 4.2; receiving phase: 1.0 M HCl; membrane composition: carrier, 60 wt%; DOP, 20 wt% and CTA, 20 wt%.

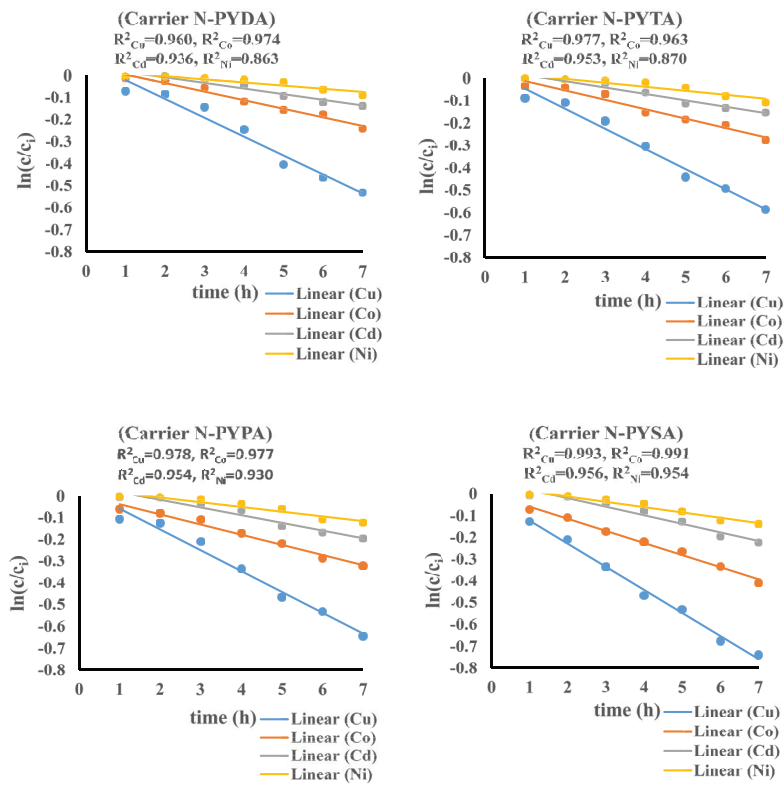Fig. 7. Kinetics of Cu(II), Co(II), Cd(II) and Ni(II) transport though PIMs containing 0.3 g of carrier, source phase: c_{Me} = 0.01 M, pH = 4.2; receiving phase = 1.0 M HCl.
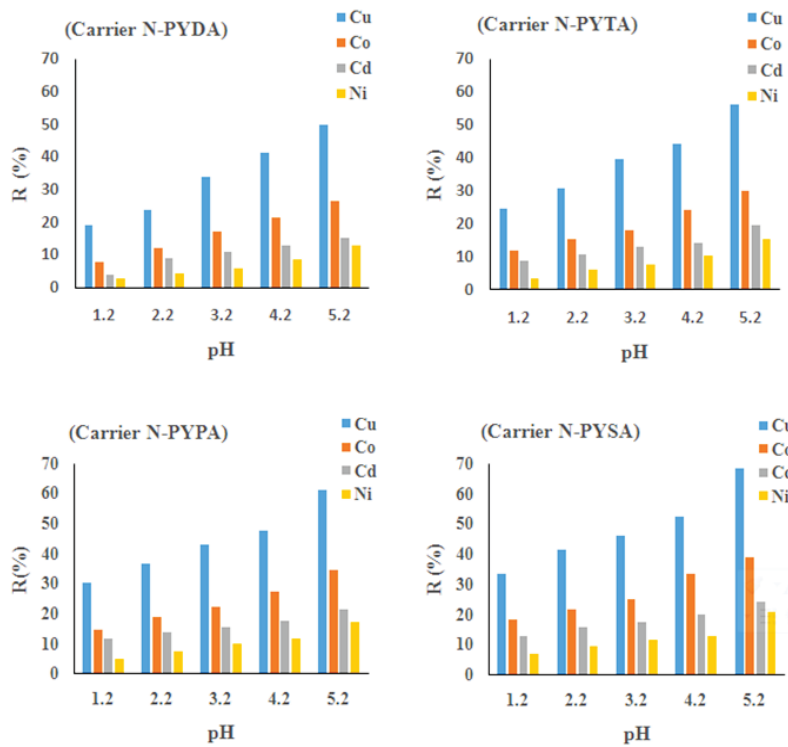

Fig. 8. Removal (%) of copper, cobalt, cadmium and nickel ions from chloride aqueous solutions in PIM transport at different pH after 7 h, 0.3 g of carrier, source phase: c_{Me} = 0.01 M and receiving phase = 1.0 M HCl.

showed that copper, cobalt, cadmium and nickel ions transport through all carriers were optimum at the pH 5.2, which achieved highest recovery of copper, cobalt, cadmium and nickel ions were 50%, 26.7%, 15.1% and 12.9%, respectively, using carrier *N*-PYDA, 56.3%, 30.1%, 19.6% and 15.5%, respectively, using carrier *N*-PYTA, 61.1%, 34.4%, 21.4% and 17.2%, respectively, using carrier *N*-PYPA, whereas carrier *N*-PYSA recorded highest removal for copper, cobalt, cadmium and nickel ions at highest pH were 68.2%, 38.7%, 24.1% and 20.6%, respectively.

The results present in Table 4 revealed that the highest initial flux for copper, cobalt, cadmium and nickel ions through PIMs using different carriers were recorded at pH 5.2. Carrier *N*-PYDA recorded 6.2×10^{-5}, 2.8×10^{-5}, 1.5×10^{-5} and 1.2×10^{-5} mol/m² s, respectively, whereas carrier *N*-PYTA recorded 7.5×10^{-5}, 3.2×10^{-5}, 2×10^{-5} and 1.5×10^{-5} mol/m² s, respectively. Carrier *N*-PYPA recorded 8.5×10^{-5}, 3.8×10^{-5}, 2.2×10^{-5} and 1.7×10^{-5} mol/m² s, respectively, whereas carrier *N*-PYSA recorded 10.3×10^{-5}, 4.4×10^{-5}, 2.5×10^{-5} and 2.1×10^{-5} mol/m² s, respectively. The obtained results showed that copper(II) ions were transported with a highest rate and selectivity order as follows: Cu(II) > Co(II) > Cd(II) > Ni(II). The initial flux of copper(II) transport increased with different carriers in the order: carrier *N*-PYDA < carrier *N*-PYTA < carrier *N*-PYPA < carrier *N*-PYSA. The highest value of the initial flux for Cu(II) ions was equal to 10.3×10^{-5} mol/m² s (for carrier *N*-PYSA) at pH 5.2.

3.3.3. Effect of membrane composition

The composition and normalized values of initial flux using different carriers characterizing the membranes used in the processes are shown in Table 5. The best results of initial flux and recovery are obtained for CTA membranes containing 40% of all carriers. In case of CTA membranes, the transport parameters of copper, cobalt, cadmium and nickel ions increased with increasing the carrier content up to 40% and decrease for higher content above 40% for all used carriers. At 40%, content of carriers recorded highest recovery for competitive transport of Cu(II), Co(II), Cd(II) and Ni(II) were 62.6%, 33.6%, 20.5% and 14.6%, respectively, for carrier *N*-PYDA, whereas carrier *N*-PYTA recorded 65.5%, 36.2%, 25.8% and 19.8%, respectively, and carrier *N*-PYPA recorded 70.6%, 40.5%, 28.1% and 22.4%, respectively. The best results were recorded for competitive transport of Cu(II), Co(II), Cd(II) and Ni(II) for carrier *N*-PYSA which recorded 76.7%, 45.6%, 30.3% and 25.8%, respectively. Results show that CTA membranes containing 40% of each carrier have highest selectivity for Cu(II) ions, whereas decreased for higher content above 40% for all used carriers. Also, data revealed that selectivity of Cu(II) ions decreased for higher content of the carriers. Transport through PIMs can be strongly influenced by the membrane morphology. In certain cases, a high concentration of carrier may result in a crystalline thin film characterized by distinctively separate layers [30–32].

Table 4
Initial flux and selectivity coefficients for competitive transport of Cu(II), Co(II), Cd(II), and Ni(II) ions at different pH using different carriers across PIMs

pH	Metals	$J_i \times 10^5$ (mol/m² s)				$S_{\text{Cu(II)/Me(II)}}$			
		Carrier 1	Carrier 2	Carrier 3	Carrier 4	Carrier 1	Carrier 2	Carrier 3	Carrier 4
1.2	Cu(II)	1.9	2.7	3.2	3.7	Cu < Co < Cd < Ni	Cu < Co < Cd < Ni	Cu < Co < Cd < Ni	Cu < Co < Cd < Ni
	Co(II)	0.7	1.2	1.4	1.8	2.7 4.8 9.5	2.3 3.4 9.0	2.3 2.9 6.4	2.1 3.1 5.3
	Cd(II)	0.4	0.8	1.1	1.2				
	Ni(II)	0.2	0.3	0.5	0.7				
2.2	Cu(II)	2.4	3.3	4.1	4.8	Cu < Co < Cd < Ni	Cu < Co < Cd < Ni	Cu < Co < Cd < Ni	Cu < Co < Cd < Ni
	Co(II)	1.2	1.5	1.9	2.2	2.0 3.0 6.0	2.2 3.3 5.5	2.2 3.2 5.9	2.2 3.2 5.3
	Cd(II)	0.8	1.0	1.3	1.5				
	Ni(II)	0.4	0.6	0.7	0.9				
3.2	Cu(II)	3.9	4.5	5.0	5.5	Cu < Co < Cd < Ni	Cu < Co < Cd < Ni	Cu < Co < Cd < Ni	Cu < Co < Cd < Ni
	Co(II)	1.7	1.8	2.3	2.6	2.3 3.6 6.5	2.5 3.8 6.4	2.1 3.3 5.0	2.1 3.2 5.0
	Cd(II)	1.1	1.2	1.5	1.7				
	Ni(II)	0.6	0.7	1.0	1.1				
4.2	Cu(II)	4.8	5.3	5.8	6.7	Cu < Co < Cd < Ni	Cu < Co < Cd < Ni	Cu < Co < Cd < Ni	Cu < Co < Cd < Ni
	Co(II)	2.2	2.5	2.9	3.7	2.2 4.0 6.0	2.1 3.8 5.3	2.0 3.2 5.3	1.8 3.4 5.6
	Cd(II)	1.2	1.4	1.8	2.0				
	Ni(II)	0.8	1.0	1.1	1.2				
5.2	Cu(II)	6.2	7.5	8.5	10.3	Cu < Co < Cd < Ni	Cu < Co < Cd < Ni	Cu < Co < Cd < Ni	Cu < Co < Cd < Ni
	Co(II)	2.8	3.2	3.8	4.4	2.2 4.1 5.2	2.3 3.8 5.0	2.2 3.9 5.0	2.3 4.1 4.9
	Cd(II)	1.5	2.0	2.2	2.5				
	Ni(II)	1.2	1.5	1.7	2.1				

Conditions: 0.3 g of carrier; source phase: c_{Me} = 0.01 M; receiving phase: 1.0 M HCl, carrier 1: N-PYDA, carrier 2: N-PYTA, carrier 3: N-PYPA and carrier 4: N-PYSA.

Table 5
Optimization of membrane ingredients to study kinetics parameters, flux, recovery and selectivity coefficient for competitive transport of Cu(II), Co(II), Cd(II) and Ni(II) ions across PIM using different carriers

| Membrane composition | | | Metal ions | $J_i \times 10^5$ (mol/m² s) | | | | R (%) | | | | $S_{Cu(II)/Me(II)}$ | | | | |
| CTA (%) | DOP (%) | Carrier (%) | | Carrier | | | | Carrier | | | | Carrier | | | | |
				1	2	3	4	1	2	3	4	1	2	3	4	
60	20	20	Cu(II)	2.4	3.2	3.9	4.5	23.8	30.1	34.9	39.6	Cu(II) < Co(II) < Cd (II) < Ni(II)	Cu(II) < Co(II) < Cd (II) < Ni(II)	Cu(II) < Co(II) < Cd (II) < Ni(II)	Cu(II) < Co(II) < Cd (II) < Ni(II)	
			Co(II)	1.3	1.7	2.1	2.7	13.7	17.2	20.6	25.8	1.9	1.9	1.9	1.7	
			Cd(II)	0.7	1.1	1.4	1.9	7.5	11.6	14.2	18.7	3.4	2.9	2.8	2.4	
			Ni(II)	0.3	0.6	1.0	1.3	3.4	6.8	10.3	13.7	8.0	5.3	3.9	3.5	
40	20	40	Cu(II)	8.9	9.6	11.0	12.9	62.6	65.5	70.6	76.1	Cu(II) < Co(II) < Cd (II) < Ni(II)	Cu(II) < Co(II) < Cd (II) < Ni(II)	Cu(II) < Co(II) < Cd (II) < Ni(II)	Cu(II) < Co(II) < Cd (II) < Ni(II)	
			Co(II)	3.7	4.0	4.7	5.5	33.6	36.2	40.5	45.6	2.4	2.4	2.3	2.4	
			Cd(II)	2.1	2.7	3.0	3.3	20.5	25.8	28.1	30.3	4.2	3.6	3.7	3.9	
			Ni(II)	1.4	2.0	2.3	2.7	14.6	19.8	22.4	25.8	6.4	4.8	4.8	4.8	
20	20	60	Cu(II)	6.2	7.5	8.5	10.3	50	56.3	61.1	68.2	Cu(II) < Co(II) < Cd (II) < Ni(II)	Cu(II) < Co(II) < Cd (II) < Ni(II)	Cu(II) < Co(II) < Cd (II) < Ni(II)	Cu(II) < Co(II) < Cd (II) < Ni(II)	
			Co(II)	2.8	3.2	3.8	4.4	26.7	30.1	34.4	38.7	2.2	2.3	2.2	2.3	
			Cd(II)	1.5	2.0	2.2	2.5	15.1	19.6	21.4	24.1	4.1	3.8	3.9	4.1	
			Ni(II)	1.2	1.5	1.7	2.1	12.9	15.5	17.2	20.6	5.2	5.0	5.0	4.9	

Conditions: Source phase: c_{Me} = 0.01 M, pH = 5.2; receiving phase: 1.0 M HCl, carrier 1: N-PYDA, carrier 2: N-PYTA, carrier 3: N-PYPA and carrier 4: N-PYSA.

Table 6
Initial flux and removal (%) for competitive transport of Cu(II), Co(II), Cd(II) and Ni(II) ions in different receiving phases using different carriers across PIMs

Receiving phase	Metal ions	$J_i \times 10^5$ (mol/m^2 s)				R (%)			
		Carrier 1	Carrier 2	Carrier 3	Carrier 4	Carrier 1	Carrier 2	Carrier 3	Carrier 4
Water	Cu(II)	3.7	4.1	4.7	5.5	33.3	36.5	40.7	45.5
	Co(II)	1.2	1.5	1.7	2.2	12.9	15.5	17.4	21.3
	Cd(II)	0.4	0.6	0.7	0.9	4.4	6.0	7.8	9.1
	Ni(II)	0.1	0.3	0.4	0.6	1.5	2.9	4.4	6.3
H$_2$SO$_4$ (1.0 M)	Cu(II)	6.8	7.1	8.5	9.4	53	54.6	60.9	64.7
	Co(II)	2.6	3.1	3.6	4.2	24.8	29.3	32.7	37.4
	Cd(II)	1.4	1.9	2.1	2.4	14.2	18.7	20.5	23.1
	Ni(II)	0.9	1.1	1.3	1.7	9.3	11.2	13.2	17.0
HNO$_3$ (1.0 M)	Cu(II)	7.8	8.1	9.9	11.1	57.7	59.5	66.6	70.9
	Co(II)	3.1	3.5	3.9	4.8	29.3	31.8	35.3	41.0
	Cd(II)	1.8	2.1	2.3	2.7	17.8	20.9	22.7	25.6
	Ni(II)	1.2	1.5	1.9	2.2	12	15.5	18.9	21.8
HCl (1.0 M)	Cu(II)	8.9	9.6	11.0	12.9	62.6	65.5	70.6	76.1
	Co(II)	3.7	4.0	4.7	5.5	33.6	36.2	40.5	45.6
	Cd(II)	2.1	2.7	3.0	3.3	20.5	25.8	28.1	30.3
	Ni(II)	1.4	2.0	2.3	2.7	14.6	19.8	22.4	25.8

Conditions: Source phase: c_{Me} = 0.01 M, pH = 5.2; membrane composition: 40 wt% carrier, 20 wt% DOP and 40 wt% CTA, carrier 1: N-PYDA, carrier 2: N-PYTA, carrier 3: N-PYPA and carrier 4: N-PYSA.

This morphology was found to be unfavorable for transport in PIMs and was often associated with poor target solute fluxes [30–32].

3.3.4. Type of receiving phase

The permeability of the membrane system for Cu(II), Co(II), Cd(II) and Ni(II) ions is considerably dependent on the nature of receiving agent for Cu(II), Co(II), Cd(II) and Ni(II) ions used in the receiving phase (Table 6). In the presence of HCl in the receiving phase, 62.8%, 33.6%, 20.5% and 14.6% of Cu(II), Co(II), Cd(II) and Ni(II) ions transport, respectively, through the membrane during 7 h using carrier *N*-PYDA, 65.5%, 36.2%, 25.8% and 19.8% of Cu(II), Co(II), Cd(II) and Ni(II) ions transport, respectively, through the membrane using carrier *N*-PYTA, 70.6%, 40.5%, 28.1% and 22.4% of Cu(II), Co(II), Cd(II) and Ni(II) ions transport, respectively, through the membrane using carrier *N*-PYPA, whereas 76.1%, 45.6%, 30.3% and 25.8% of Cu(II), Co(II), Cd(II) and Ni(II) ions transport, respectively, through the membrane using carrier *N*-PYSA. Results show that the highest flux for all carriers favors when the receiving medium is HCl (Table 6), whereas Cu(II) ions recorded highest flux through different carriers using HCl as receiving phase as follows 8.9 × 10^{-5}, 9.6 × 10^{-5}, 11 × 10^{-5} and 12.9 × 10^{-5} mol/m^2 s, respectively, for carriers (*N*-PYDA, *N*-PYTA, *N*-PYPA and *N*-PYSA). Using water as receiving phase showed the lowest percentage for Cu(II), Co(II), Cd(II) and Ni(II) ions transport through different membranes using different carriers. This lower percentage may be due to weak complexing ability than membrane complex constituents. This makes lower in rate constant and flux in comparison with HCl, HNO$_3$ and H$_2$SO$_4$.

Table 7
Removal (%) for competitive transport of Cu(II), Co(II), Cd(II) and Ni(II) ions in different concentration of receiving phase using different carriers across PIMs

Concentration of HCl	Metal ions	R (%)			
		Carrier 1	Carrier 2	Carrier 3	Carrier 4
1.0	Cu(II)	62.6	65.5	70.6	76.1
	Co(II)	33.6	36.2	40.5	45.6
	Cd(II)	20.5	25.8	28.1	30.3
	Ni(II)	14.6	19.8	22.4	25.8
2.0	Cu(II)	65.3	68.8	76.8	83.4
	Co(II)	38.1	39.8	41.5	47.7
	Cd(II)	22.7	26.7	30.0	32.5
	Ni(II)	17.4	22.5	25.3	27.4
3.0	Cu(II)	69.8	71.5	80.7	90.0
	Co(II)	40.5	42.7	44.1	49.4
	Cd(II)	24.1	27.2	31.6	34.2
	Ni(II)	18.9	23.6	26.5	28.1

Conditions: Source phase: c_{Me} = 0.01 M, pH = 5.2; membrane composition: 40 wt% carrier, 20 wt% DOP and 40 wt% CTA, receiving phase: HCl, carrier 1: *N*-PYDA, carrier 2: *N*-PYTA, carrier 3: *N*-PYPA and carrier 4: *N*-PYSA.

3.3.5. Effect of different concentrations of receiving phase

The recovery of Cu(II), Co(II), Cd(II) and Ni(II) ions transport for all carriers was recorded at different concentration of HCl ranging from 1.0 to 3.0 M. Table 7 showed that highest recovery for all metals was recorded at optimum concentration 3.0 M of HCl for all carriers. Which carrier

N-PYSA showed highest recovery for copper ions reached to 90% at 3.0 M of HCl.

4. Conclusion

The PIMs containing amides derived from 4-aminoantipyrine and fatty acids as ion carriers and DOP as the plasticizer provide an attractive alternative to conventional solvent extraction methods for the separation of Cu(II), Co(II), Cd(II) and Ni(II) ions. The results showed that Cu(II) can be effectively recovered from aqueous acidic chloride solutions containing Co(II), Cd(II) and Ni(II) ions in hydrometallurgical process of transport across the PIM with amides. The PIM containing amides with different fatty chain influenced the rate of transport of copper, cobalt, cadmium and nickel ions, which length of alkyl fatty chain increased the rate of transport increased. The highest flux of copper(II) ions was obtained by transport through the PIM containing 40 wt% carrier, 20 wt% DOP and 40 wt% CTA. The obtained results showed that recovery of Cu(II) ions reached to 90% into 3.0 M hydrochloric acid as the receiving phase after 7 h using carrier *N*-PYSA. Finally, the developed in this work system can be useful for recovery of Cu(II) from acidic aqueous solutions containing Co(II), Cd(II) and Ni(II) ions.

References

[1] R.A. Bartsch, J. Way, Chemical Separation with Liquid Membranes, ACS Symposium Series 642, Washington, D.C., USA, 1996, pp. 575–579.
[2] A.J.B. Kemperman, H.H.M. Rolevink, D. Bargeman, T.V.D. Boomgaard, H. Strathmann, Stabilization of supported membranes by interfacial polymerization top layers, J. Membr. Sci., 138 (1998) 43–55.
[3] S. Kim, S.K. Kim, M.H. Cho, S.H. Lee, J.Y. Kim, S. Kwon, E.H. Lee, Permeation of silver ion through polymeric CTA membranes containing acyclic polyether bearing amide and amine end group, Bull. Korean Chem. Soc., 22 (2001) 1076–1080.
[4] J. Kozlowska, C.A. Kozlowski, J.J. Koziol, Transport of Zn(II), Cd(II), and Pb(II) across CTA plasticized membranes containing organophosphorous acids as an ion carriers, Sep. Purif. Technol., 57 (2007) 430–434.
[5] J. Gyves, A.M. Hernández-Andaluz, R. De San Miguel, LIX®-loaded polymer inclusion membrane for copper(II) transport, J. Membr. Sci., 268 (2006) 142–149.
[6] B. Pośpiech, W. Walkowiak, Separation of copper(II), cobalt(II) and nickel(II) from chloride solutions by polymer inclusion membranes, Sep. Purif. Technol., 57 (2007) 461–465.
[7] M. Kołodziejska, C.A. Kozłowski, M. Ulewicz, Separation of lead(II) and copper(II) by plasticizer membranes with sulphuranalogus of phosphinic acids as carriers, Physicochem. Prob. Miner. Process., 49 (2012) 267–276.
[8] B. Gajda, A. Skrzypczak, M.B. Bogacki, Separation of cobalt(II), nickel(II), zinc(II) and cadmium(II) ions from chloride solution, Physicochem. Prob. Miner. Process., 46 (2011) 289–294.
[9] S.D. Kolev, Y. Baba, R.W. Cattrall, Solid phase extraction of zinc(II) using a PVC-based polymer inclusion membrane with di(2-ethylhexyl)phosphoric acid (D2EHPA) as the carrier, Talanta, 78 (2009) 795–799.
[10] M. Ulewicz, U. Lesińska, M. Bocheńska, Facilitated transport of Zn(II), Cd(II) and Pb(II) ions through polymer inclusion membranes with calix[4]-crown-6 derivatives, Sep. Purif. Technol., 54 (2007) 299–305.
[11] O. Arous, F.S. Saoud, A. Mourad, H. Kerdjoudj, Efficient facilitated transport of lead and cadmium across a plasticized triacetate membrane mediated by D2EHPA and TOPO, Mater. Sci. Appl., 2 (2011) 615–623.
[12] C.A. Kozłowski, J. Kozłowska, W. Pellowski, W. Walkowiak, Separation of cobalt-60, strontium-90, and cesium-137 radioisotops by competitive transport across polymer inclusion membranes with organophosphorus acids, Desalination, 198 (2006)149–156.
[13] C.A. Kozłowski, Facalitated transport of metal ions through composite and polymer inclusion membranes, Desalination, 198 (2006) 140–148.
[14] S. Kanemaru, T. Oshima, Y. Baba, Solid–liquid extraction and transport of metal ion with the polymer inclusion membrane using a new alkylated pyrrolidine carboxylic acid, J. Chem. Eng. Jpn., 45 (2012) 816–822.
[15] C.I. Gherasim, G. Bourceanu, R. Olariu, C. Arsene, A novel polymer inclusion membrane applied in chromium (VI) separation from aqueous solutions, J. Hazard. Mater., 197 (2011) 244–253.
[16] J.A. Riggs, B.D. Smith, Facilitated transport of small carbohydrates through plasticized cellulose triacetate membranes. Evidence for fixed-site jumping, J. Am. Chem. Soc., 119 (1997) 2765–2766.
[17] B.D. Smith, S.J. Gardiner, T.A. Munro, Facilitated transport of carbohydrates, catecholamines, and amino acids through liquid and plasticized organic membranes, J. Inclusion Phenom. Mol. Recognit. Chem., 32 (1998) 121–131.
[18] T.A. Munro, B.D. Smith, Facilitated transport of amino acids by fixed-site jumping, Chem. Commun., 22 (1997) 2167–2168.
[19] J.A. Calzado, C. Palet, M. Valiente, Facilitated transport and separation of aromatic amino acids through activated composite membranes, Anal. Chim. Acta, 431 (2001) 59–67.
[20] M. Matsumoto, T. Takagi, K. Kondo, Separation of lactic acid using polymeric membrane containing a mobile carrier, J. Ferment. Bioeng., 85 (1998) 483–487.
[21] M. Matsumoto, Y. Murakami, Y. Minamidate, K. Kondo, Separation of lactic acid through polymer inclusion membranes containing ionic liquids, Sep. Sci. Technol., 47 (2012) 354–359.
[22] Y. Sakai, R.W. Cattrall, I.D. Potter, S.D. Kolev, R. Paimin, Transport of thiourea through an aliquat 336/polyvinyl chloride membrane, Sep. Sci. Technol., 35 (2000) 1979–1990.
[23] L.D. Nghiem, P. Mornane, I.D. Potter, J.M. Perera, R.W. Cattrall, S.D. Kolev, Extraction and transport of metal ions and small organic compounds using polymer inclusion membranes (PIMs), J. Membr. Sci., 281 (2006) 7–41.
[24] M. Ulewicz, J. Szczygelska-Tao, J.F. Biernat, Transport of Zn(II), Cd(II) and Pb(II) across polymer inclusion membrane doped with imidazole azocrown ethers, Desalination, 214 (2007) 352–364.
[25] N.S. Murthy, S.T. Correal, H. Minor, Structure of the amorphous phase in crystallisable polymers: poly(ethylene terephtalate), Macromolecules, 24 (1991) 1185–1189.
[26] G. Vancso, D. Snetvy, I. Tomka, Structural changes during polystyrene orientation: a study of optical birefringence and wide angle X-ray scattering, J. Appl. Polym. Sci., 42 (1991) 1351–1359.
[27] C. Fontas, R. Tayeb, S. Tingry, M. Hidalgo, P. Seta, Transport of platinum(IV) through supported liquid membrane (SLM) and polymeric plasticized membrane (PPM), J. Membr. Sci., 263 (2005) 96–102.
[28] R. Tayeb, C. Fontas, M. Dhahbi, S. Tingry, P. Seta, Cd(II) transport across supported liquid membranes (SLM) and polymeric plasticized membranes (PPM) mediated by Lasalocid A, Sep. Purif. Technol., 42 (2005) 189–193.
[29] Y.M. Scindia, A.K. Pandey, A.V.R. Reddy, Coupled-diffusion transport of Cr(VI) across anion-exchange membranes prepared by physical and chemical immobilization methods, J. Membr. Sci., 249 (2005) 143–152.
[30] A. Gherrou, H. Kerdjoudj, R. Molinari, P. Seta, Preparation and characterization of polymeric plasticized membranes (PPM) embedding a crown ether carrier application to copper ions transport, Mater. Sci. Eng., C, 25 (2005) 436–443.
[31] A. Gherrou, H. Kerdjoudj, R. Molinari, P. Seta, E. Drioli, Fixed sites plasticized cellulose triacetate membranes containing crown ethers for silver(I), copper(II) and gold(III) ions transport, J. Membr. Sci., 228 (2004) 149–157.
[32] O. Arous, H. Kerdjoudj, P. Seta, Comparison of carrier-facilitated silver(I) and copper(II) ions transport mechanisms in a supported liquid membrane and in a plasticized cellulose triacetate membrane, J. Membr. Sci., 241 (2004) 177–185.